Numerical Modelling of the Refraction of Wind Wave Spectra on the Southern Brazilian Coast

José Henrique G. M. Alves[1] and Eloi Melo[2]

[1]School of Mathematics, UNSW, 2052 Sydney, NSW, Australia
[2]Depto. de Engenharia Sanitaria e Ambiental, UFSC, Brazil

Two numerical models are used to calculate wind wave spectrum transformations in an area of the Southern Brazilian Coast exposed to the South Atlantic Ocean. Using shallow water measurements made at a single point of frequency directional spectra recorded during the arrival of a swell event, estimates of the deep water, spatially homogeneous spectra are made using an inverse refraction model. The deep water spectrum is then forward propagated by using a second spectral refraction model based on a different set of governing equations, providing information about the wave field throughout a numerical grid covering an extensive area. The performance of the forward refraction model is assessed by comparing the numerical calculations to analytical and experimental data.

1. INTRODUCTION

Wind waves are the main source of energy driving coastal dynamics. Before reaching the shore, waves propagate through the continental shelf, ongoing transformations that result from several physical processes. This paper presents a numerical modelling approach to assess wave propagation in a small area of the Southern Brazilian Coast using original directional measurements of the wave field.

The basic problem addressed here is: how to obtain information about the wave spectra throughout a wide area using single point measurements of the wave field close to the shore? The solution of the problem involves two main steps.

First, estimates of the wave spectrum in a region where it is approximately homogeneous in space are obtained. For the purposes of the present study, this happens in "deep-water", defined as the region where the depth exceeds half the typical wavelengths of the considered spectrum. Since the available measurements are made close to the shore, where the depths are much smaller than that threshold, the estimation of a deep-water spectrum requires the inverse propagation of the wave field from shallow to deep water — inverse propagation.

The second step is to obtain estimates of the wave field in a wide area comprised between deep water and the shoreline, which includes the surroundings of the measurement site — forward propagation. This is achieved using a simple spectral refraction model based on two conditions derived from the ray theory (Munk & Arthur, 1951). The numerical model used to estimate the deep water spectrum is described in detail by O'Reilly (1991). Since the forward propagation involves a numerical model specifically developed within the context of the present study, it will be described in more detail below. A complete description can also be found in Alves (1996).

2. GENERAL THEORY

Longuet-Higgins (1955, 1956) shows that the transformation through refraction of the energy initially concentrated around an arbitrary surface area of the directional wind wave spectrum keeps itself related to the same frequency throughout the entire transformation process. Therefore, it is possible to establish a direct relationship between an initially undisturbed spectral energy distribution $E_0(f,\theta_0)df\,d\theta$ and the distribution after the wave field has undergone refraction $E(f,\theta)df\,d\theta$, as long as dissipation and diffraction can be neglected.

The governing equation relating the initial and the refracted spectrum is

$$E(f,\theta) = \frac{k}{k_0}\frac{c_{g0}}{c_g} E_0(f,\Gamma(f,\theta)) \qquad (1)$$

where the directional spectrum has been discretized into components with frequency f, direction of propagation θ, wave number k and group velocity c_g, following the assumption that the principle of linear superposition is valid. The subscripts 0 denote properties related to the spectrum before refraction. The wave numbers and group velocities are related to the wave frequency through the dispersion relation for small amplitude waves. The gamma function $\Gamma(f,\theta)$ on the r.h.s. of equation (1) relates initial and refracted directions

$$\theta_0 = \Gamma(f,\theta). \qquad (2)$$

Equation (1) is valid along a ray path, which itself defines the gamma function (equation 2). For an orthogonal Cartesian frame, the ray equations (Munk & Arthur, 1951) are

$$\frac{dx}{dt} = c_g \cos\theta \qquad (3)$$
$$\frac{dy}{dt} = c_g \sin\theta$$
$$\frac{d\theta}{dt} = \frac{dc_g}{dx} sin\theta - \frac{dc_g}{dy} cos\theta$$

Equation (1) is used presently to calculate the deep water spectrum $E_0(f,\theta_0)df\,d\theta$ given a measured spectrum in shallow water. Since the procedure is done reversing the natural sequence, it is called inverse refraction. Techniques based on equation (1) are also called spectral mapping (see e.g., O'Reilly, 1991; O'Reilly & Guza, 1996).

Properties of the wave field in a large area including the surroundings of the measurement site are calculated using two other properties derived from the ray theory. Changes in the wave length of each spectral component due to refraction are calculated by applying the wave number irrotationality condition

$$\nabla \times k = 0. \qquad (4)$$

Wave height variations due to refraction are calculated through the energy flux conservation equation

$$\nabla \bullet \left(c_g A^2\right) = 0 \qquad (5)$$

where A is the amplitude (half the wave height) of a given spectral component.

The numerical solution of the coupled system of equations (4) and (5) allows for the use of grids covering large computational domains. A numerical model that solves equations (4) and (5)is described in details next.

3. FORWARD REFRACTION MODEL

A spectral wind wave refraction model based on the methodology firstly applied by Dalrymple (1988) to study monochromatic wave propagation is used. The spectral model is based on the coupled system of equations (4) and (5), which are solved explicitly using a finite difference method.

The numerical solution is built on a discretization module shifted in the y direction, resembling a zig-zag shape (Figure 1). The solution progresses in y from left to right or vice-versa depending on the initial direction θ of each component at the outer boundary. The whole spectrum is solved after the discretization module has swept all grid points for a fixed x position. The solution progresses in the x axis, aligned cross-shore, line by line.

For a Cartesian system of reference, equation (4) can be rewritten as

$$\frac{\partial A_n}{\partial x} - \frac{\partial B_n}{\partial y} = 0 \qquad (6)$$

where $A_n = k_y = k_n \sin\theta_n$ and $B_n = k_x = k_n \cos\theta_n$ are the orthogonal projections of the wave number modulus k_n. The subscript n, which refers to an arbitrary component of the directional frequency spectrum $E(f,\theta)$, will be dropped from the following equations for the sake of simplicity. By definition, B can be related to A by

$$B = \left(k^2 + A^2\right)^{1/2} \qquad (7)$$

The wave number modulus is related to the frequency by the dispersion relation $\omega = (gk \tanh kh)^{1/2}$, where g is the acceleration due to gravity and h is the local water depth. Therefore, the wave number is calculated directly from the frequency at each grid point considering only the local depth.

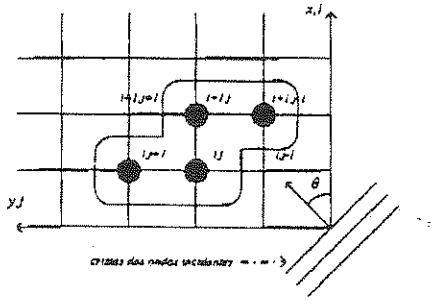

Figure 1: Detail of the numerical mesh and of the discretization module. The slashes on the lower right corner illustrate wave crests

Equation (6) is discretized using central differences along the x and y axis, with equally spaced intervals Δx and Δy. The partial differentials in x are solved at an intermediate point $(i+1/2, j)$. The resulting expressions for the x and y partial derivatives are

$$\left(\frac{\partial B}{\partial y}\right) = r\left[B_{i,j+1} - B_{i,j} + B_{i+1,j} - B_{i+1,j-1}\right] \qquad (8)$$

and

$$A_{i+1,j} = A_{i,j} + r\left[B_{i,j+1} - B_{i,j} + B_{i+1,j} - B_{i+1,j-1}\right] \qquad (9)$$

where $r = \Delta x/2\Delta y$. Using the relation (7) it is possible to eliminate the B terms with subscript $(i+1, j)$, which identify unknown quantities. After some algebra, the resulting expression is

$$A_{i+1,j}^2 + 2bA_{i+1,j} + c = 0 \qquad (10)$$

where

$$b = \frac{\left[r\left(B_{i+1,j-1} - B_{i,j+1} + B_{i,j}\right) - A_{i,j}\right]}{\left(1 + r^2\right)} \qquad (11)$$

and

$$c = \frac{\left[\left(\left(1+r^2\right)b\right)^2 - r^2 k_{i+1,j}^2\right]}{\left(1+r^2\right)} \qquad (12)$$

The positive root of equation (10) gives the solution for the A terms at each new grid point as the solution progresses in space. The B terms are obtained directly through the relation (7). The angle of propagation at each grid point is, therefore

$$\theta_{i,j} = \tan^{-1}\left(\frac{A_{i,j}}{B_{i,j}}\right) \qquad (13)$$

The numerical solution of the energy conservation equation (5) is obtained similarly. Using equation (6), now with $A = Ec_g \cos\theta$ and $B = -Ec_g \sin\theta$, the resulting expressions to be solved are

$$A_{i+1,j} = \frac{A_{i,j} + r\left[B_{i+1,j-1} - B_{i,j+1} + B_{i,j}\right]}{1 + r\left(\frac{\sin\theta_{i+1,j}}{\cos\theta_{i+1,j}}\right)} \qquad (14)$$

and

$$B_{i+1,j} = A_{i+1,j}\left(\frac{\sin\theta_{i-1,j}}{\cos\theta_{i+1,j}}\right) \qquad (15)$$

where the group velocity is given by

$$c_g = \frac{d\omega}{dk} = \frac{g}{2k}\tanh kh\left(1 + \frac{2kh}{\sinh 2kh}\right) \qquad (16)$$

The numerical model outputs amplitude and angle of propagation of individual spectral components. Since the entire spectrum is solved progressing line by line toward the x direction, it is also possible to compute statistical parameters of the wave field at each grid point. The main parameter used for applications is the significant wave height H_s, obtained from the model calculations through the expression

$$H_s = \left(2\Sigma\left(H_n\right)_{i,j}^2\right)^2 \qquad (17)$$

where the wave height H_n of individual components is defined by

$$\left(H_n\right)_{i,j} = \frac{8\left(A_n\right)_{i,j}}{c_g \cos\left(\theta_n\right)_{i,j}} \qquad (18)$$

and A is the energy flux in the x direction (equation 14).

Two tests were made to assess the model performance. The first compared the analytical solution of monochromatic wave propagation with several angles of incidence over a beach with plane parallel depth contours (see e.g. Dean & Dalrymple, 1984) to the model calculations. Throughout all the test cases the model produced the exact analytical solution.

The second test compared the model results with those from a laboratory experiment made by Mase & Kirby (1992). In this case, a spectrum was propagated over a beach with plane parallel depth contours. An algorithym to calculate wave breaking based on statistical properties of the wave field as proposed by Thornton and Guza (1983) was included to provide the energy decay at the surf zone.

The comparison made at 12 equally spaced points along the domain in the x direction are summarised in Figure 2. Before the onset of breaking — locations 1 to 8 — experiment and model agree with less than 5% relative error. The agreement is still good at locations 9 (0.43%) and 10 (5.02%), therefore inside the breaking zone. Locations 11 and 12 have 19% and 57% errors, respectively, probably due to non-linear effects not included in the model.

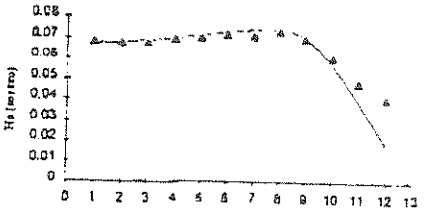

Figure 2. Comparison between laboratory results from Mase & Kirby [1992] (triangles) and model calculation (continuous line)

4. RESULTS

To address the problem posed above, four frequency-direction spectra representing different stages of a swell event recorded at the measurement site on September 1996 are used. The spectra were discretized into 12 frequency bands with 30 directional bins each. The inverse refraction model used a rectangular 186 km by 185 km grid with $\Delta x = \Delta y = 250m$. Using the inverse refraction model (O'Reilly, 1991) based on equations (1) to (3), deep water spectra were obtained for each of the four cases considered. They are the initial, two intermediate and the final spectra of the swell event.

Figure 3 shows an example of the differences between the shallow water, measured spectrum of an intermediate stage of the event and its correspondent deep water estimate. The remarkable difference indicates the importance of refraction to modifying properties of the wave field in the study site. Considering the four cases, the differences in significant wave height between shallow and deep water were always greater than 20%.

The deep water spectra were then used as initial conditions for the forward propagation model. A new rectangular 136km (x direction) by 185km (y direction) depth grid with $\Delta x = \Delta y = 250m$ was used. The resulting

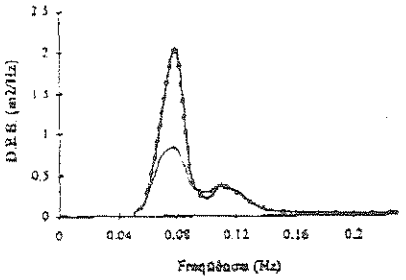

Figure 3: Shallow water (line with circles) and deep water (simple line) frequency spectra

calculated field of significant wave height agreed qualitatively well with visual observations of wave height in different areas of the domain.

A quantitative assessment of the complete methodology used to estimate the wave field in a wide area using point measurements, consisting of a comparison between the measured and the forward propagated spectrum at the measuring point, is also presented here. This might seem an obvious comparison, but it is worthwhile stressing that even though the inverse refraction and forward propagation models are based on the same physical assumptions, they are developed using on different mathematical approaches, as outlined in Section 1.

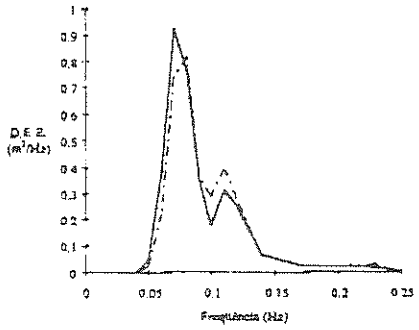

Figure 4: Comparison between measured (dashed line) and calculated (continuous line) frequency spectra for swell on 8th of September of 1996, 7:00AM

Comparisons between the measured and calculated directionally integrated (one-dimensional) frequency spectra show excellent agreement, with differences in significant wave height less than 4%. Figure 4 illustrates the comparison between measured and calculated frequency spectra for the case with strongest refraction (Sept 8/1996, 7AM). A comparison of the directional structure is also presented in Figure 5 for the same case. Note that the calculated directional distribution (continuous line) reproduces well the measured distribution (dashed line), even without smoothing of the calculated data.

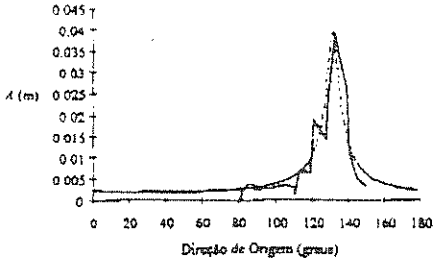

Figure 5: Directional distribution of amplitudes at the peak frequency. Spectrum measured on 8th of September of 1996, at 7:00AM. Measured (dashed line) and calculated (continuous line) are shown.

5. CONCLUDING REMARKS

A methodology for studying wind wave spectra transformation by refraction is proposed and applied to an area of the Southern Brazilian Coast. The objective is to reconstruct the wave field along wide areas using single point directional measurements of the wave spectrum. The methodology consists of two parts:

- Calculation of the deep water spectrum using an inverse refraction model and
- Reconstruction of the wave field along a wide area using a spectral refraction model, which is presented and successfully tested against analytical and experimental data.

Considering the study site, comparisons between measured and calculated spectra show that the methodology produces good results.

The methodology presented here is based on numerical models developed using simple approaches to the problem of the transformation of wind wave spectrum in shallow waters. Therefore, the computational cost involved in its application, that can be extended to a wide range of beaches with simple bottom reliefs, is considerably low and attractive. Several limitations arise from the assumptions of linearity of the wave spectrum. However, these can reduced through proper modifications and extensions of the governing equations used above.

ACKNOWLEDGEMENTS

The authors gratefully acklowledge the support from the Conselho Nacional de Desenvolvimento Cientifico e Tecnologico (CNPq). Brazil. We also thank Dr. William O'Reilly, from the University of Berkeley, USA, for providing the inverse refraction code, and Dr. Jose Antonio Lima, from Cenpes/Petrobras, for his useful suggestions.

REFERENCES

Alves, J.H.G.M., *Refracao do espectro de ondas oceanicas em aguas rasas. aplicacoes a regiao costeira de Sao Francisco do Sul, SC*, MSc Thesis, Dept. Engenharia Sanitaria e Ambiental/UFSC, 89 pp., Brazil, 1996.

Dalrymple, R.A., Model for refraction of water waves. *J. Waterways, Port, Coastal and Ocean Engineering*, 114, 423-435, 1988.

Dean, R.G. and Dalrymple, R.A. *Water wave mechanics for engineers and scientists*, World Scientific, 4th Edition, 353 pp., Singapore, 1984.

Longuet-Higgins, M.S., The refraction of sea waves in shallow water, *Journal of Fluid Mechanics*, 1, 163-176, 1955.

Longuet-Higgins, M.S., On the transformation of a continuous spectrum by refraction. *Proc. Cambridge Phyl. Soc.*, 53(1), 226-229, 1956.

Mase, H. and Kirby, J.T, Modified frequency-domain KdV equation for random wave shoaling. *Proc. 23rd ICCE*, Venice, 474-487, 1992.

Munk, W.H and Arthur, R.S., Wave intensity along a refracted ray. *Scripps Institute of Oceanography Wave Report*, 95, Ref. 51-7, 18 pp., 1951.

O'Reilly, W. *Modelling surface gravity waves in the Southern California Bight*, PhD Thesis, Scripps Institute of Oceanography/UCSD, 89 pp., San Diego, 1991.

O'Reilly, W. and Guza, R.T., Assimilating coastal wave observations in regional swell predictions. Part 1: Inverse methods, *J. Phys. Oceanography*, submitted in 1996.

Thornton, E.B. and Guza, R.T., Transformation of wave height distribution. *J. Geophys. Res.*, 88(C10), 5925-5938, 1983.